

Table captions

Table S1. Typical characterizations of the frozen hydrometeor classes.

		Diameter (mm)	Density (g cm^{-3})	Terminal velocity (m s^{-1})
Cloud ice	Columnar crystals	0.01—1 ⁽¹⁾	0.36—0.7 ⁽²⁾	0.013—0.055 ⁽²⁾
	Plate-like	0.01—1 ⁽¹⁾	~0.9 ⁽¹⁾	0.02—0.06 ⁽²⁾
	Dendrites	0.1—3 ⁽¹⁾	0.3—1.4 ⁽¹⁾	0.25—0.7 ⁽³⁾
Snowflakes		2—5 ⁽¹⁾	0.05—0.89 ⁽¹⁾	0.5—3 ⁽¹⁾
Graupel		0.5—5 ⁽¹⁾	~0.4 ⁽¹⁾	3—14 ⁽¹⁾
Hail		5—80 ⁽¹⁾	0.8—0.9 ⁽¹⁾	10—40 ⁽¹⁾

⁽¹⁾ Pruppacher H.R. (1978).

⁽²⁾ Jayaweer and Ryan (1972).

⁽³⁾ Mitchell and Heymsfield (2005).

Figure captions

Fig. S1. The 110×100 grid points in the computational domain.

Fig. S2. Profiles of temperature (black line) and relative humidity (red line) from atmospheric radiosonde launched near Edmonton, Alberta on 29 May 2001.

Fig. S3. Probability distribution function of vertical velocities (w) at cloud base layer under different fire forcing conditions (a); Relationship between input fire forcing (FF) and induced vertical velocity (w) at cloud base (b). The aerosol concentration is $1,000 \text{ cm}^{-3}$. The shaded area represents the variability of estimation ($\pm 1/2\sigma$).

Fig. S4. Contributions of individual frozen hydrometeor to total frozen water content under four extreme conditions , which are referred to as (1) LULA: low updrafts ($2,000 \text{ W m}^{-2}$) and low aerosols (200 cm^{-3}); (2) LUHA: low updrafts ($2,000 \text{ W m}^{-2}$) and high aerosols ($100,000 \text{ cm}^{-3}$); (3) HULA: high updrafts ($300,000 \text{ W m}^{-2}$) and low aerosols (200 cm^{-3}); (4) HUHA: high updrafts ($300,000 \text{ W m}^{-2}$) and high aerosols ($100,000 \text{ cm}^{-3}$).

Fig. S5. Time evolution of surface rain rates for the three aerosol episodes ($N_{\text{CN}} = 200$; $1,000$; and $100,000 \text{ cm}^{-3}$ respectively) under LU (low updrafts, $FF=2,000 \text{ W m}^{-2}$) and HU (high updrafts, $FF=50,000 \text{ W m}^{-2}$) conditions.

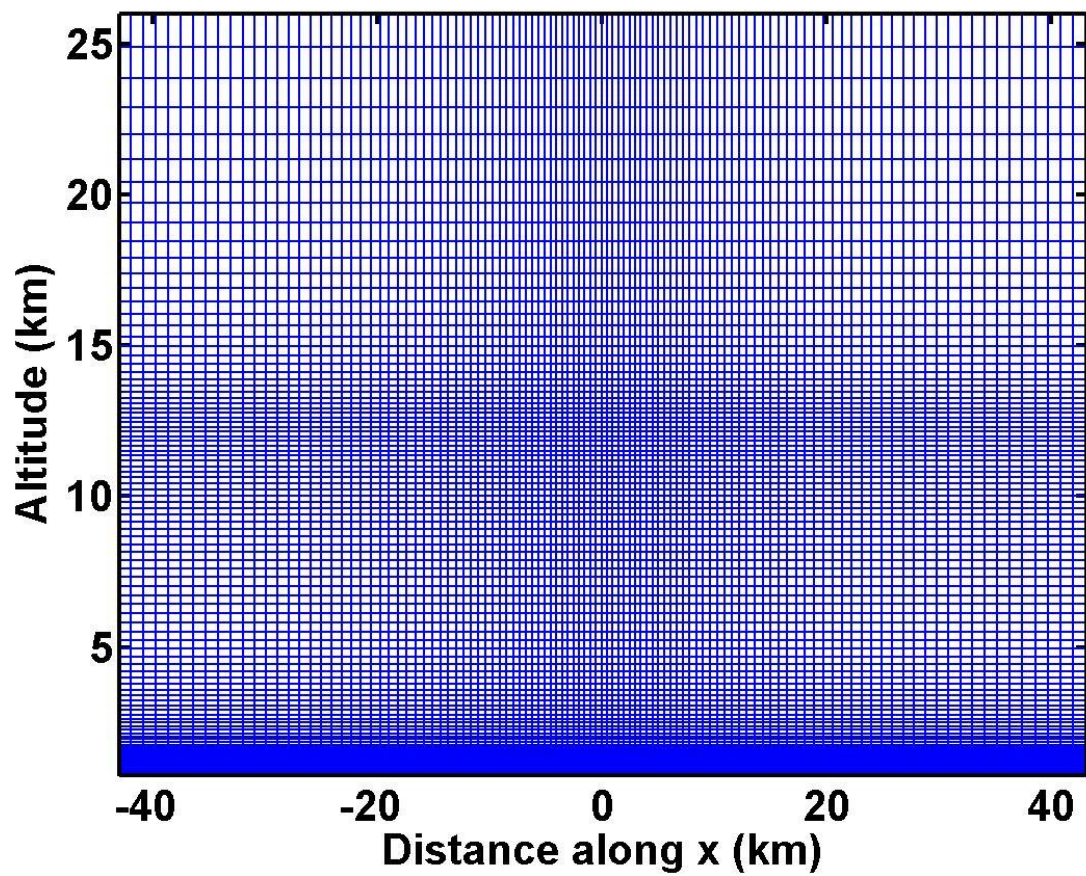


Fig. S1. The 110×100 grid points in the computational domain.

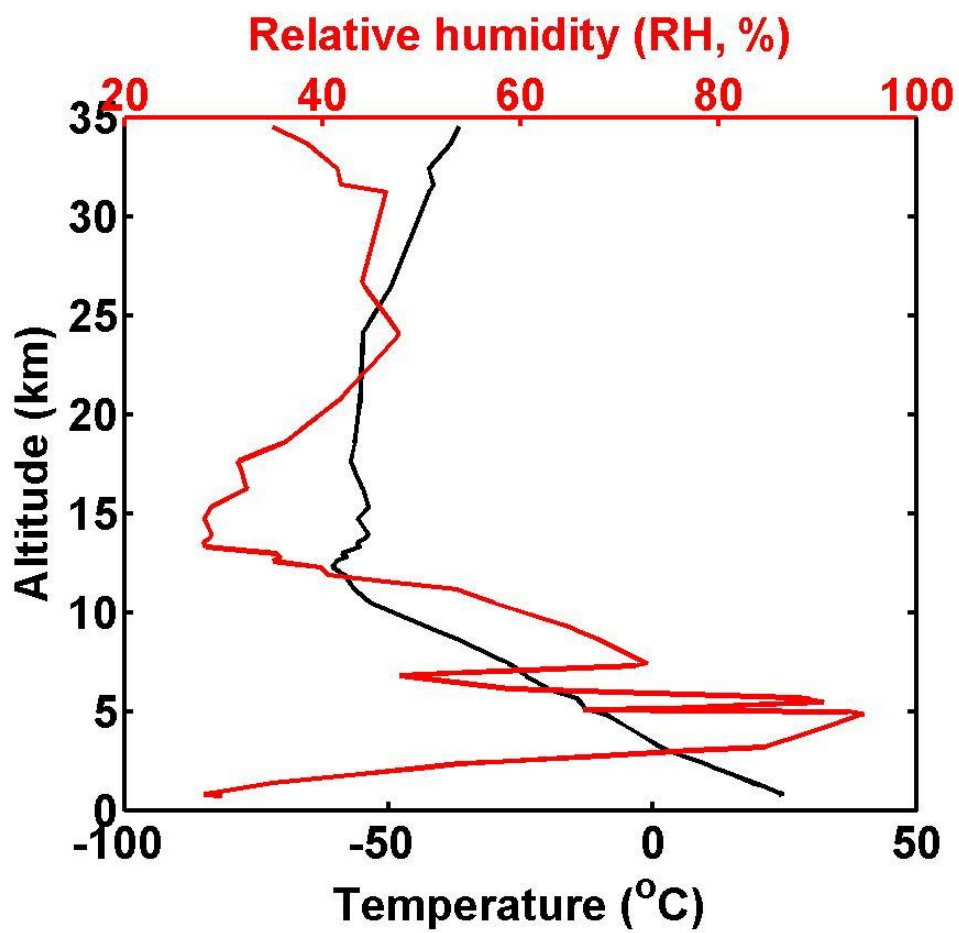


Fig. S2. Profiles of temperature (black line) and relative humidity (red line) from atmospheric radiosonde launched near Edmonton, Alberta on 29 May 2001.

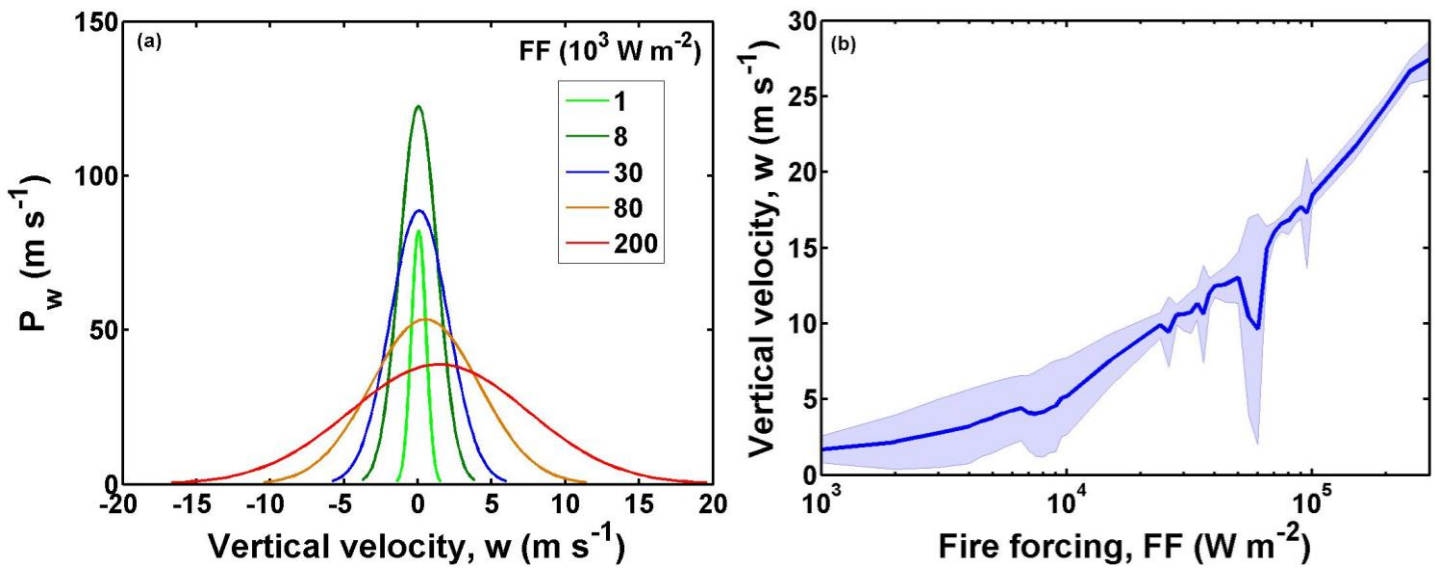


Fig. S3. Probability distribution function of vertical velocities (w) at cloud base layer under different fire forcing conditions (a); Relationship between input fire forcing (FF) and induced vertical velocity (w) at cloud base (b). The aerosol concentration is $1,000 \text{ cm}^{-3}$. The shaded area represents the variability of estimation ($\pm 1/\sqrt{2}\sigma$).

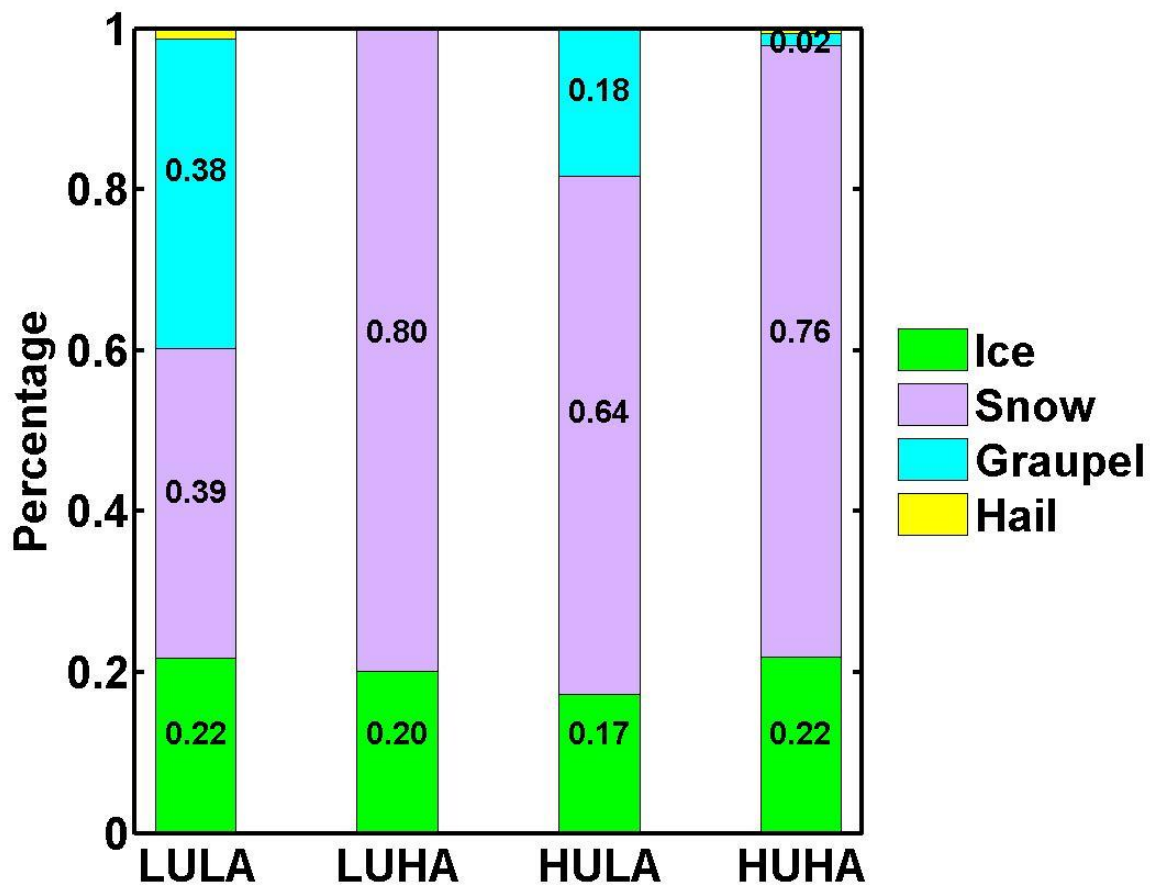


Fig. S4. Contributions of individual frozen hydrometeor to total frozen water content under four extreme conditions which are referred to as (1) LULA: low updrafts ($2,000 \text{ W m}^{-2}$) and low aerosols (200 cm^{-3}); (2) LUHA: low updrafts ($2,000 \text{ W m}^{-2}$) and high aerosols ($100,000 \text{ cm}^{-3}$); (3) HULA: high updrafts ($300,000 \text{ W m}^{-2}$) and low aerosols (200 cm^{-3}); (4) HUHA: high updrafts ($300,000 \text{ W m}^{-2}$) and high aerosols ($100,000 \text{ cm}^{-3}$).

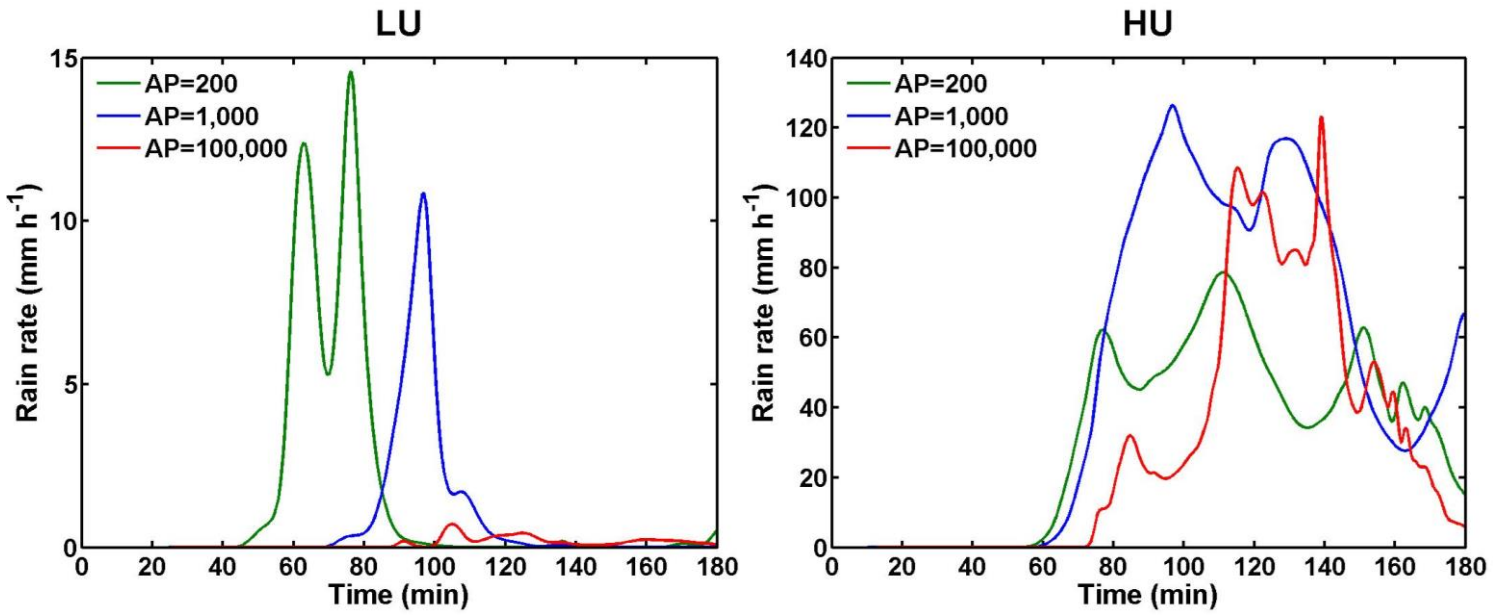


Fig. S5. Time evolution of surface rain rates for the three aerosol episodes ($N_{\text{CN}} = 200$; 1,000; and 100,000 cm^{-3} respectively) under LU (low updrafts, $FF=2,000 \text{ W m}^{-2}$) and HU (high updrafts, $FF=50,000 \text{ W m}^{-2}$) conditions.

References

- Jayaweer, K., and Ryan, B. F.: Terminal Velocities of Ice Crystals, Q J Roy Meteor Soc, 98, doi: 10.1002/qj.49709841516, 1972.
- Mitchell, D. L., and Heymsfield, A. J.: Refinements in the treatment of ice particle terminal velocities, highlighting aggregates, J Atmos Sci, 62, 1637-1644, doi: 10.1175/Jas3413.1, 2005.
- Pruppacher H.R., K. J. D.: Microphysics of Clouds and Precipitation, D. Reidel, 1978.